PCCP

Spot the difference: hydrogen adsorption and dissociation on unsupported platinum and platinum-coated transition metal carbides

Journal:	*Physical Chemistry Chemical Physics*
Manuscript ID	CP-ART-06-2021-002974.R1
Article Type:	Paper
Date Submitted by the Author:	12-Aug-2021

Complete List of Authors:	Koverga, Andrey; Universidad de Medellin, Facultad de Ciencias Básicas Florez, Elizabeth; Universidad de Medellin, Facultad de Ciencias Basicas Jimenez-Orozco, Carlos; Universidad de Medellin, Facultad de Ciencias Básicas Rodriguez, Jose; Brookhaven National Laboratory, Chemistry Division

Spot the difference: hydrogen adsorption and dissociation on unsupported platinum and platinum-coated transition metal carbides

Andrey A. Koverga[a*], Elizabeth Flórez[a], Carlos Jimenez-Orozco[a*], José A. Rodriguez[b]

[a]Grupo de Investigación Mat&mpac, Facultad de Ciencias Básicas, Universidad de Medellín, Medellín 050026, Colombia.

[b]Chemistry Division, Brookhaven National Laboratory, Upton, NY 11973, United States

Corresponding authors

E-mail addresses: akoverga@unal.edu.co (A. Koverga), cjimenez@udem.edu.co (C. Jimenez-Orozco)

Abstract

Hydrogenation reactions are involved in several processes in heterogeneous catalysis. Platinum is the best-known catalyst, however, there are limitations to its practical use. Therefore, it is necessary to explore alternative materials and transition metal carbides (TMC) have emerged as potential candidates. We explore the viability of using cheap TMC as supports for a Pt monolayer, aiming to reduce the amount of the noble metal in the catalyst without a significant loss of its activity towards H_2 dissociation. Hence, analyzing H_2 dissociation from a fundamental point of view is a necessary step towards a further practical catalyst. By means of periodic DFT calculations, we analyze H_2 adsorption and dissociation on Pt/β-Mo_2C and Pt/α-WC surfaces, as a function of hydrogen surface coverage (Θ_H), resembling a more realistic model of a catalyst. H_2 dissociation rates were analyzed as a function of the reaction temperature. The results show that Pt/C-WC and Pt/Mo-Mo_2C have a Pt-like behavior for H_2 dissociation at Θ_H>1/2 ML. At a particular temperature of 298 K, Pt/C-WC and Pt/Mo-Mo2C have low energy barriers for H_2*→2H* (0.13 and 0.11 eV, respectively), close to the value of Pt (0.06 eV). For the highest coverage, i.e. Θ_H =1, Pt/C-WC has a lower activation energy and a higher reaction rate than Pt. Finally, the H_2 dissociation rate is higher in Pt/Mo-Mo_2C than in Pt, when rising the temperature above 298 K. Our results put Pt/C-WC and Pt/Mo-Mo_2C under the spotlight as a potential catalyst for H_2 dissociation, with a similar performance than Pt, paving the way for further experimental and/or theoretical studies, addressing the capability of Pt/TMC as practical catalysts in hydrogenation reactions.

Keywords:

Hydrogen; dissociation; DFT; kinetics; surface; coverage

1 Introduction

Hydrogenation reactions are extremely important in the field of *green* energy; however, in their majority they are not possible without an efficient catalyst, usually being a platinum-group metal.[1] The main problem with platinoid metals (i.e. Pt, Os, Ru, Rh, Pd and Ir) is their extreme scarcity and high market prices, preventing an efficient commercialization of catalyst-based hydrogenation processes.

To tackle this obstacle and to reduce the price of the catalytic hydrogenation processes, it is necessary to either completely eliminate the usage of platinum or, at the very least, decrease its active loading in the catalysts. Transition metal carbides (TMC), known to have catalytic properties similar to Pt,[2-4] are potential candidates to solve this problem. Indeed, the transition metals such as titanium, tantalum, tungsten, molybdenum and vanadium are significantly more abundant than platinum-group metals[5] and, as a result, their prices are orders of magnitude lower than those of the noble metals.[6] Such a difference in prices suggests that the replacement or reduction by loading the platinoid metals on catalytic devices with a TMC, offers a great opportunity for cost reduction of catalyzed hydrogenation processes.

Practically, the main bulk of an active catalyst can be replaced with a TMC by deploying platinum nanoparticles onto the support, similarly to the preparation of a catalyst active towards the hydrogen evolution reaction.[7]

This method, however, has a clear disadvantage since the core part of the nanoparticle remains unexposed to the environment, and thus it is underutilized. To overcome this drawback, it is possible to deposit a monolayer of platinum onto the support, thus further optimizing loading of the active catalyst.[7]

Among the possible TMC supports, tungsten carbide (WC) and molybdenum carbide (Mo_2C) represent a good choice due to closeness of their electronic and structural properties to those of Pt-group materials.[2,8]

Hydrogenation processes of unsaturated hydrocarbons on Pt-based catalysts often involve adsorption and dissociation of molecular hydrogen on the surface.[9,10] Therefore, understanding how molecular and atomic hydrogen interacts on a fundamental level with platinum-based materials, can contribute to the design of useful hydrogen storage devices and fuel cells.

Hydrogen interaction with pure platinum has been studied extensively, both experimentally[11-15] and theoretically;[16-20] also a detailed analysis of atomic hydrogen adsorption on TMC-supported platinum systems (Pt/TMC) was reported in our previous work.[21] However, a systematic fundamental study of adsorption and dissociation of H_2 on these complex surfaces is still required to gain a better idea about the perspectives of these materials for being used as active catalysts for energy storage and conversion solutions. In this regard, significant

advances in computational power have enabled accurate and cost-effective theoretical approaches useful to design materials for electrocatalytic applications based on density functional theory (DFT).[22,23]

Since hydrogenation processes typically take place in an environment rich in hydrogen,[24,25] and hydrogen tends to adsorb dissociatively on platinum surfaces,[14,15,26-28] it is also important to understand the role of hydrogen surface coverage on the interaction of H_2 with Pt/TMC systems.

Thus, the goal of the present work is to gain insights into the H_2 interaction with Pt/TMC on a fundamental level. In particular, molecular hydrogen adsorption and dissociation on platinum monolayers supported on tungsten and molybdenum carbides (Pt/WC and Pt/Mo_2C, respectively) have been investigated with and without pre-adsorbed atomic hydrogen on them, for modelling hydrogen surface coverage at different regimes, similar to a previous work for clean TMC surfaces.[9] It is noteworthy that there is a certain disagreement in the notation of the TMC crystal structure in the literature. Here, we use the notation proposed by Kurlov and Gusev for WC,[29] while for Mo_2C we follow the nomenclature defined by the Joint Committee on Powder Diffraction Standards (JCPDS).[8] Thus, here we consider a (0001) surface of the hexagonal phase of tungsten carbide, α-WC(0001),[30] and a (100) surface of orthorhombic molybdenum carbide, β-Mo_2C (100),[31] as supports for a Pt. Specifically, due to the notable differences in the adlayer—substrate interaction, depending on whether the carbon or metal termination of the TMC is in direct contact with the supported metal,[21,32-35] Pt monolayers supported on polar metal and carbon terminations of WC and Mo_2C were studied.

In this work, the kinetics of H_2 dissociation have been explored by determining the dissociation barrier heights at several hydrogen surface coverages. Furthermore, the effect of the temperature on the dissociation reaction rates has been considered. The Pt(111) surface with the closest geometry to supported Pt monolayers, and frequently used in fundamental studies of hydrogenation reactions,[36] was used as a benchmark system to compare all the results obtained for the Pt/TMC systems.

2 Computational details

Periodic density functional theory calculations were performed using the Vienna *ab initio* simulation package (VASP).[37,38] The generalized gradient approximation proposed by Perdew, Burke and Ernezerhof for the exchange-correlation energy functional[39] was used. It must be said here that a correct choice of an exchange-correlation functional may not be a trivial task, since theoretically calculated reaction barrier heights can be sensitive to the selected functional.[40-42]

A benchmark study conducted for gas-phase reactions involving hydrogen revealed that pure GGA functionals provide results comparable to meta-GGA results and somewhat worse than barriers obtained using hybrid functionals.[40] At the same time, while hybrid functionals and meta-GGA functionals undeniably provide

results closer to the experimentally observed ones,[40,41] their application to surface chemistry has been rather limited due to both high computational cost and poor description of metallic systems.[43] The PBE functional, on the other hand, has proven to be a good choice for theoretical description of Pt-[44,45] and TMC-based systems[9,46] and their interaction with various adsorbates.

Valence electron density was expanded in a plane-wave basis set and the effects caused by the core electrons on the valence region were described by the Projector Augmented Wave (PAW) method by Blöchl[47] as implemented in VASP by Kresse and Joubert.[48] A Kinetic energy cut-off of 415 eV for the plane wave basis set was defined, which is sufficient to obtain reproducible and reliable results on systems with carbides[8,49] and carbides-supported metals.[50,51] To include the long-range correlation effects,[52] van der Waals (vdW) correction proposed by Grimme,[53] specifically its D3 scheme[54] was used, being an appropriate method for TMC-based systems as previously reported.[9,46]

Throughout all the calculations, dipole corrections were included to prevent dipole coupling between images of the unit cell repeating in the direction perpendicular to the surface plane. The reciprocal space for all surfaces was approximated with the 3 × 3 × 1 Monkhorst-Pack scheme.[55] The Methfessel-Paxton approach[56] with a Gaussian width of smearing of 0.2 eV was used for the Fermi level smearing.

The carbide surfaces (both carbon- and metal-terminated, respectively) in this work referred to as C-WC, C-Mo_2C, W-WC and Mo-Mo_2C, were represented by (4 × 4) supercells, each of them comprised of two metal and two carbon alternating atomic layers[21,46]. A vacuum region of not less than 13 Å was added to each cell to prevent interactions between repeating images in the *z* direction of the slab.

The Pt monolayer (ML) supported on each transition metal carbide (TMC) was modeled by completely covering the support with platinum atoms, as reported in our previous work[21] (See Fig. 1). Therefore, sixteen Pt atoms were present in each Pt/TMC system. For structure optimization calculations of Pt/TMC surfaces, the platinum layer was allowed to relax simultaneously with the upper two atomic layers of the support, while two remaining layers were frozen to represent bulk of the support (1+2+2 approach). Adsorbates, present on the surface, were allowed to relax in all three directions as well.

The surface sites considered for H_2 adsorption on Pt/TMC were the same as described in our previous work for atomic hydrogen bonding and are labeled following an identical notation[21] (Fig. 1). A platinum ML supported on α-WC, regardless the support's termination, has a high symmetry similar to that of a Pt(111) surface; thus, typical sets of top, bridge and hollow sites were considered for the Pt/WC systems. On Pt/β-Mo_2C, the adsorption sites, although similar by nature to those on Pt/WC, were not as symmetric due to the lower symmetry of the Pt/β-Mo_2C system, as seen in Fig. 1.

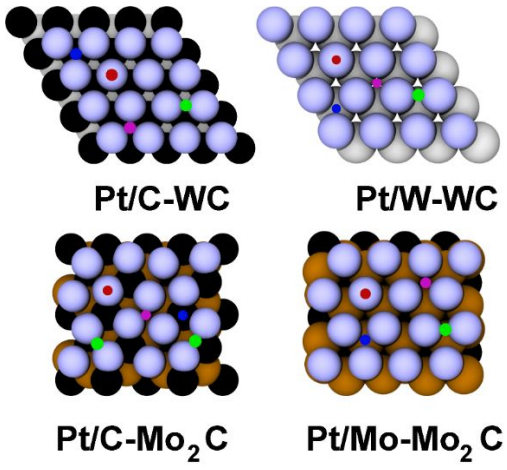

Fig. 1. Adsorption sites available for H_2 bonding on the Pt/TMC surfaces. Black, silver and ocher spheres represent carbon, tungsten and molybdenum atoms, respectively. Platinum atoms are represented by pale blue spheres. Top, bridge, E*hcp* and C/Mo/W*hcp* hydrogen sites are indicated by red, green, purple and blue dots, respectively.

Molecular hydrogen adsorption energies, dissociation barriers and rates of the dissociation processes were studied at different hydrogen coverages (Θ_H) of the Pt/TMC surfaces, considering several pre-adsorbed H atoms, for which the adsorption sites have been established in our previous work.[21] The coverage was calculated as a ratio between the sum of total number of H atoms in the system (belonging to both molecular and atomic hydrogen) and sixteen platinum atoms. Thus, the following models were considered: a) single H_2 molecule present on Pt/TMC surfaces without atomic H, where Θ_H = 1/8 ML; b) Pt/TMC surfaces with six atoms of hydrogen and H_2 molecule, here coverage was Θ_H = 1/2 ML; c) surfaces with fourteen H atoms and H_2 molecule, where coverage was Θ_H = 1 ML.

Adsorption energies for molecular hydrogen on Pt/TMC surfaces were obtained from expression:

$$E_{Ads,H} = E_{Tot} - E_{surf} - E_{H_2,g} + \Delta E_{ZPE} \qquad (1)$$

In Eq (1), E_{Tot}, E_{Surf} and $E_{H_2,g}$ are energies of the system with the adsorbate on the surface, of the surface with the geometry before H_2 adsorption, and of the isolated hydrogen molecule in vacuum, respectively. The term ΔE_{ZPE} relates to the difference between zero-point energy (ZPE) contributions to the electronic energy for E_{Tot} and $E_{H2,g}$ systems. Hence, ΔE_{ZPE}=ZPE(E_{Tot}) + ZPE($E_{H2,g}$). The general form for every ZPE contribution (E_{ZPE}) can be expressed as

$$E_{ZPE} = \sum_{i=1}^{nvf} (1/2) h\nu_i \qquad (2)$$

h here is Planck's constant and ν_i corresponds to the normal vibrational frequencies (nvf).

The vibrational frequencies were calculated using a harmonic approximation, considering exclusively vibrational frequencies of the adsorbate in vacuum, ZPE ($E_{H2,g}$), and the adsorbed hydrogen (both H and H_2, ZPE(E_{Tot})). They were obtained from the diagonalization of the Hessian matrix with finite difference elements computed through analytical gradients with displacements of the coordinates of the involved atoms of 0.01 Å.

To investigate the $H_2 \rightarrow 2H$ process on the studied surfaces, the energy barriers were calculated using the climbing image nudged elastic band (CI-NEB) method, as implemented in VASP by Henkelman, Uberuaga and Jónsson,[57] and Henkelman and Jónsson.[58]

The most stable geometries of H_2-Pt/TMC were used as initial states (IS) for the CI-NEB calculations, while stable 2H-Pt/TMC systems were considered as final states (FS), for the case of Θ_H=1/8. At this lowest coverage no stable adsorption site was found for H_2 on Pt(111), thus the dissociation on this surface was studied using the IS, where the H_2 molecule was located at the distance of 3.20 Å, not directly interacting with platinum. A similar procedure was carried out for the other coverages. Four intermediate system images between the IS and FS were generated and used to locate the saddle point under the condition that total forces acting on the elastic band were no larger than 0.01 eV $Å^{-1}$. Each obtained TS structure was verified using frequency analysis, where the transition state was confirmed by checking for the existence of a single imaginary frequency.

Energy barrier (E_a) values were then calculated as

$$E_a = (E_{TS} + ZPE_{TS}) - (E_{IS} + ZPE_{IS}) \qquad (3),$$

where E_{TS} and E_{IS} are the total energies of the transition and initial states, respectively, and ZPE_{TS} and ZPE_{IS} are their respective ZPE contributions.

Reaction energies for H_2 dissociation were calculated as the difference between the energies of the product and reactant, accounting for the respective ZPE contributions for both of these terms:

$$\Delta E = (E_{FS} + ZPE_{FS}) - (E_{IS} + ZPE_{IS}) \qquad (4)$$

In equation 4 E_{FS} and E_{IS} are the total energies of the final (two H atoms) and initial (H_2 molecule) states, respectively. The same applies for other coverages different from Θ_H=1/8.

It is important to highlight that the barriers and the reaction energies were calculated at the same surface coverage. Thus, for Θ_H=1/8 ML, the initial system was represented by a single H_2 molecule on the surface, and the transition and final states, by two H atoms on the same surface. Calculations at Θ_H=1/2 ML considered the H_2 molecule co-adsorbed with six H atoms as the IS, while the TS and FS had a configuration where eight atoms of hydrogen were present on the surface. Finally, at the monolayer hydrogen coverage, the initial state was

represented by fourteen H atoms present on the surface simultaneously with H_2 molecule, and the surfaces completely covered with atomic hydrogen, were considered as the transition and final states.

To further analyze the dissociation process of molecular hydrogen on the Pt/TMC surfaces, the dependency of its elementary reaction rate, *r*, on temperature, *T*, was estimated using harmonic transition state theory applied to surface reactions[59,60]

$$r = \left(k_B T/h\right)\left(q_{vib}^{TS}/q_{vib}^{IS}\right)exp\left(-E_a/k_B T\right) \qquad (5)$$

here k_B is the Boltzmann constant, *T* – temperature, *h* – Plank constant, *Ea* – activation energy including ZPE contributions, q^{TS}_{vib} and q^{IS}_{vib} – the vibrational partition functions of the TS and IS, respectively.

In their turn, the vibrational partition functions can be expressed as

$$q_{vib} = \prod_{i=1}^{nvf}\left(1/(1 - exp(-h\nu/k_B T))\right) \qquad (6).$$

Translational and rotational partition functions for the IS were not accounted for, since their inclusion does not alter the observed tendencies for the hydrogen dissociation rate (See Section S1 in Supplementary Information for more details).

3 Results and discussion

3.1 Platinum monolayer interaction with α-WC(0001) and β-Mo_2C(100) supports

In our previous work[21] we demonstrated that the stability of a Pt monolayer (ML) on the TMC support can be evaluated from adsorption energy of the monolayer calculated as

$$E_{Ads} = \frac{E_{Pt+TMC} - 16 \times E_{Pt_g} - E_{TMC}}{16} \qquad (7)$$

where E_{Pt+TMC} is the total energy of the system with the Pt monolayer placed on the TMC surface, E_{Pt_g} corresponds to the energy of the isolated Pt atom in the vacuum, and E_{TMC} denotes the total energy of the pristine TMC surface. Obtained adsorption energies, indicated below in parentheses, evidence that the stability of the Pt monolayer (ML) on the TMC support decreases in the order Pt/W-WC (-7.86 eV) > Pt/Mo-Mo_2C (-7.56 eV) > Pt/C-Mo_2C (-7.22 eV) > Pt/C-WC (-6.16 eV). Strong Pt-support interactions are present in all the Pt/TMC systems: even on the C-WC support, where platinum adsorption was the weakest compared to the rest of the systems, the adsorption energy is still very negative, thus indicating high stability of the platinum ML on the α-WC(0001) and β-Mo_2C(100) supports.

The Pt/WC systems have a highly symmetric array of the platinum adlayer, similar to the geometry of Pt(111), while the platinum adlayers exhibit a significantly lower symmetry on the Mo_2C surfaces, because of the different symmetries of the support and the monolayer. This symmetry mismatch is especially evident on the C-Mo_2C terminations where the topmost C atoms of the support become embedded between the atoms of platinum. Despite this difference in the symmetries, no actual reconstruction has been reported either for WC or Mo_2C to our knowledge.

Another effect of the support on the geometry of the platinum adlayer is seen on the Pt-Pt distances in all systems, which are larger (for Pt/C-WC and Pt/W-WC by 4.3%, for Pt/C-Mo_2C by 10.6 % and for Pt/Mo-Mo_2C by 8.9 %) than in the unsupported Pt(111) surface. This elongation could have an effect on the stability of atomic hydrogen on the Pt/TMC surfaces,[35,51,61] and thus have an impact on catalytic activity of these system towards H_2 dissociation.

Additionally to the observed "strain" in the platinum adlayer, the interactions between the surface atoms and the support may result in a modification of the electronic structure of the adatoms, changing the chemical properties of platinum (termed as a ''ligand effect'' in literature[62]). Ligand effects have a defining role on the strength of the H-Pt interactions at monolayer platinum coverage;[51] therefore, it must be taken into account when evaluating the catalytic activity of these systems towards molecular hydrogen dissociation.

Thus, another important difference between platinum adlayers supported on the different terminations of WC and Mo_2C is charge distribution. In all Pt/TMC systems, with the exception of Pt/C-WC, the charge transfer takes place from the support to platinum atoms, and they become slightly oxidized. In Pt/C-WC system a small transfer Pt → WC of 0.19*e* was observed, which is the result of the presence of the exposed carbon atoms in direct contact with the supported metal in this system. Although a similar phenomenon would be expected in the Pt/C-Mo_2C system, platinum adatoms, nonetheless, draw a charge from the support through its molybdenum atoms that are in direct contact with the monolayer.

Hence, similarly to copper supported on the TMC,[34,35,50] the chemical reactivity of Pt ML is expected to change with the TMC support and its carbon and/or metal termination.

Another important characteristic of the supported platinum ML, that is also sensitive to the nature of the TMC support and its termination, is the position of its *d*-band center. Its shifts further away from the Fermi level were observed for all the Pt/TMC systems, compared to the *d*-band center of Pt(111) located at -2.58 eV,[21,63,64] although the magnitude of the shift was different for each Pt/TMC system. The *d*-band ML supported on C-WC(0001) surface was located 0.86 eV further from the Fermi level, while the shift of -0.05 eV observed for Pt/Mo-Mo_2C system was the smallest among the studied systems.

In this regard, the *d*-band model[65] suggests that the *d*-band shift toward the Fermi level, or upshift, would lead to a lower occupation of anti-bonding states in the adsorbate-surface interaction, thus increasing the stability of the adsorbate on the surface, and a shift away from the Fermi level, or downshift, would have a negative effect on the adsorbate-surface interaction. This correlation can be used to estimate changes in the catalytic properties towards selected processes for a given material relative to a reference system.[66]

Thus, changes in the geometry, electronic structure and charge distribution of platinum adlayer with the nature of the support and its termination are expected to affect catalytic properties of the resulting complex Pt/TMC systems. Hence, a systematic study of the impact of the support on the interactions of platinum adlayer with molecular hydrogen, is required, to make a conclusion about catalytic activity of Pt/TMC towards H_2 dissociation.

3.2 H_2 interaction with Pt/TMC surfaces

Here, molecular hydrogen adsorption on Pt/TMC surfaces was studied by using an initial geometry, where H_2 was placed at 2.5 Å from the surfaces in a tilted initial orientation with an angle of $\sim 40°$ relative to the surface plane. This geometry is an intermediate between a perpendicular orientation of the molecule, from which the dissociation energy barrier on Pt(111) is higher, and a completely parallel orientation from which the barrierless dissociation is possible[67].

In this work, we consider H_2 molecule as interacting with a given surface as long as there is a difference in total energy of the H_2-Pt system and the sum of total energies of isolated H_2 and Pt components even if the distances between H_2 and a surface are quite large.[68]

Interestingly, H_2 molecule placed at 2.5 Å distance from the Pt(111) surface shows a dissociative adsorption, while placing it at a distance larger than 3 Å leads to an even further increase of the H_2 – Pt distance. The total energy in the latter case is identical to the sum of the total energies of Pt(111) and H_2 in gas, therefore, evidencing that no intact hydrogen molecule adsorption taking place on this particular surface.

This dissociative adsorption of molecular hydrogen on platinum is in a disagreement with previously reported theoretical studies, which found barriers of various heights for H_2 dissociation on the pristine Pt(111).[19,20,69,70] This apparent contradiction can be attributed to the Grimme's D3 dispersion corrections used in the present work (required for these systems), but not included in the mentioned theoretical reports.

Indeed it has been shown that inclusion of the Grimme's D2 dispersion corrections has a clear impact on H_2 interaction with platinum;[70] in the same time, adsorption characteristics of atomic H (which is product of H_2 dissociation) depend also on the model parameters,[21,30] dispersion corrections among them.[71] The last mentioned work showed that inclusion of the dispersion corrections has a significant impact on energy values

for molecular and atomic hydrogen adsorption on orthorhombic molybdenum carbide. This fact is extremely important for a correct description of H_2 interaction with complex Pt/TMC surfaces, since it has been demonstrated before that at the monolayer coverage, the properties of the supported metallic adlayer do not fully resemble the properties of the corresponding bulk metal,[21,35] and the support has an impact on hydrogen adsorption characteristics.

At the same time, the dissociative adsorption seen on the model Pt(111) is also an additional evidence that selected model parameters describe adequately the H_2 interaction with this surface, because our results are in a good agreement with available experimental works[14,26-28] which report that hydrogen adsorbs dissociatively on Pt surfaces in vacuum with no significant dissociation barrier. In general, the absence of consensus on the activation barriers for H_2 dissociation on Pt has been mentioned before and is a result of the complexity of the H-Pt systems, much higher than it would be expected for such a classical subject.[13]

From a fundamental viewpoint, the absence of a barrier can be attributed to a decrease in the H—H bond strength in the molecule, resulting from filling antibonding orbitals of the gas molecule with free electrons from the surface.[72] The experimental study, mentioned above,[13] also point to the existence of a precursor state for hydrogen on Pt(111), where the molecule is trapped in a physisorption well, the depth of which is a function of hydrogen coverage. In a later work by the same authors, the decisive role of the surface defects on H_2 dissociation on Pt(111) was highlighted,[73] suggesting that on the TMC-supported platinum monolayers, less symmetrical than Pt(111), other factors may also have impact on the dissociation barrier height. Indeed, while on the supported Pt monolayers no ”traditional” defects, such as kink sites or terrace edges are present, the strain on Pt monolayer mentioned in the previous section could have an impact on the dissociation barrier height on the Pt/TMC surfaces.

On the clean Pt/TMC surfaces, H_2 also mainly adsorbs dissociatively, regardless of the support and its termination. However, its intact adsorption (without cleavage of the H—H bond) is possible as well, since at least one site was found on each TMC-supported platinum monolayer, where hydrogen adsorbs without dissociating, thus, evidencing a stabilizing nature of the presence of the support on molecular H_2 adsorption on platinum.

Analyzing molecular hydrogen adsorption energies in the Pt/TMC systems, it becomes evident that on all the Pt/TMC the most stable H_2 adsorption has been observed on top of Pt atom (Fig. 2). Notice that the intramolecular H—H distances (Table S2 in Supplementary Material, SI) are larger than 0.74 Å found in the gas phase.[74] It is important to mention here that H_2 adsorption on Pt(111) at the lowest 1/8 ML coverage is not indicated in Fig. 2 due to the fact that at this coverage not a H_2 molecule, but rather 2 H atoms are interacting with the surface.

H_2 adsorption was analyzed at different surface coverages, Θ_H, placing the H_2 molecule on top sites, while several sites were gradually occupied by atomic hydrogen, as reported previously,[21] i.e. C*hcp*, Top, C*hcp* and Mo*hcp* for Pt/C-WC, Pt/W-WC, Pt/C-Mo_2C and Pt/Mo-Mo_2C, respectively.

Importantly, as it was mentioned above, at monolayer coverages of Pt on the TMC, the interaction with atomic hydrogen is defined mainly by the nature of the carbide substrate, rather than by the supported metallic monolayer.[21,35] Therefore, while adsorption of atomic hydrogen on TMCs is a complex process, which could cause surface reconstruction in some carbides,[75,76] these effects have not been reported so far to take place for WC and Mo_2C, and thus the reconstruction of Pt/TMC surfaces with an increasing hydrogen coverage is unlikely.

For H_2 adsorption on Pt(111) at Θ_H=1/2 ML, six of its E*hcp* sites were occupied by atomic hydrogen, and molecular hydrogen adsorption was analyzed on top, bridge, E*hcp* (fcc) and hcp sites. At this coverage, the sable final geometry corresponds to H_2 located atop of Pt(111) at a distance of 3.43 Å from the surface and interacting weakly with it, evidenced by the E_{ads} of -0.32 eV. Similar geometry then was used to analyze H_2 adsorption at 1 ML hydrogen coverage on Pt(111).

The structures obtained after the relaxation procedure, together with H—H intramolecular distances and adsorption energies can be seen in Fig. 2. At the intermediate 1/2 ML coverage, hydrogen molecule is stable on Pt(111), Pt/C-WC and Pt/C-Mo_2C at a distance of around 3 Å from the surfaces (Table S2), and the H—H distance in these cases is close to 0.75 Å. On the metallic terminations of the carbide support (W-WC, Mo-Mo_2), coated with platinum, only a small increase in the Pt-H_2 distances is observed compared to that at the lowest 1/8 surface coverage (Table S2).

At the highest 1 ML Θ_H, the H—H distances in the H_2 on most of the Pt/TMC surfaces are close to 0.75 Å except for the Pt/W-WC, where it was found to be 0.83 Å. For Pt/W-WC and Pt/Mo-Mo_2C, similarly to adsorption at the intermediate coverage Θ_H=1/2 ML, the H_2—Pt distances are much smaller, compared to those on Pt/C-WC and Pt/C-Mo_2C.

At both intermediate 1/2 ML and highest 1 ML coverages, these changes in H_2—Pt distances are mainly the result of the rising occupation of the Pt/TMC (or Pt(111)) surface sites by atomic hydrogen and its repulsive interaction with the H_2 molecule in their proximity.

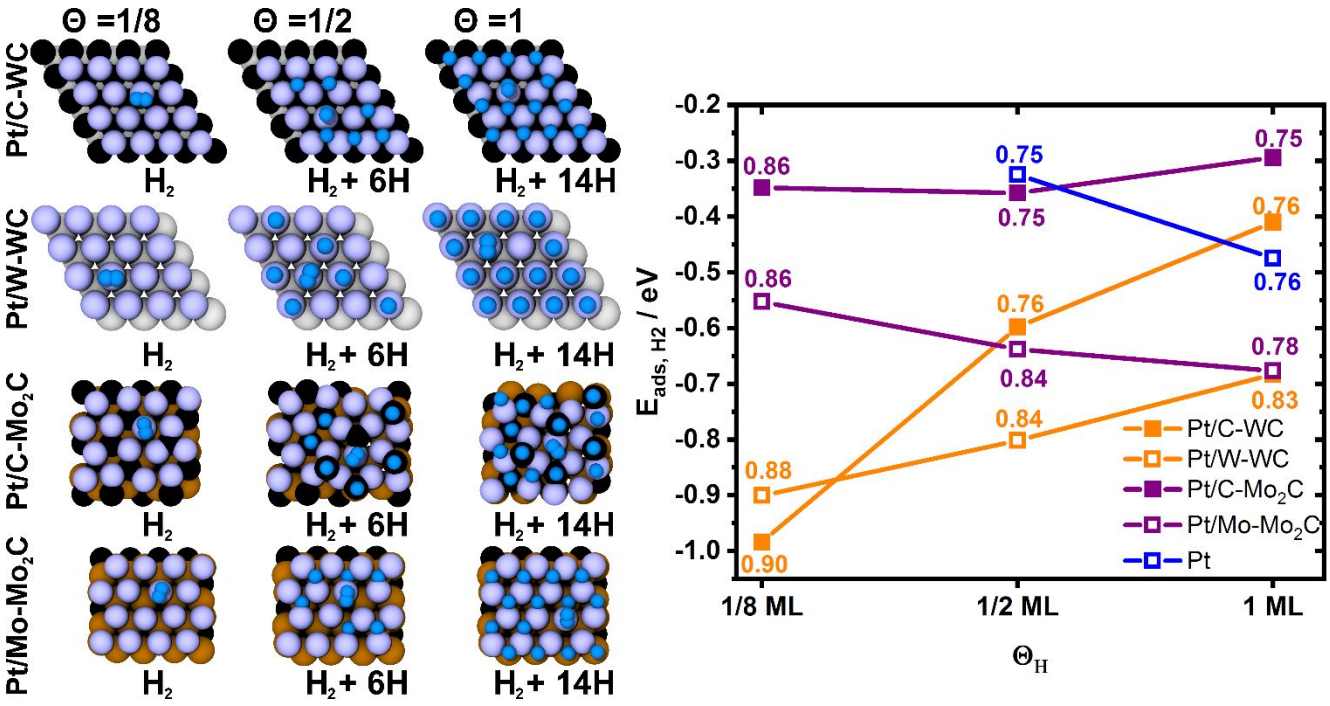

Fig. 2. Left panel: Stable geometries for the H_2 molecule on the Pt/α-WC(0001) and Pt/β-Mo_2C surfaces after geometry relaxation at different Θ_H. Spheres' color code is the same as in Fig. 1. Dark blue spheres represent H atoms. Right panel: Variation in hydrogen adsorption energy as a function of hydrogen coverage on the Pt/TMC and Pt(111)surfaces. Numbers at each point indicate the respective H—H intramolecular distance (in Å unit).

The adsorption energy values in Fig. 2 show that on all the Pt/TMC surfaces, except on Pt/Mo-Mo_2C, a destabilization of the H_2 molecule takes place with growing Θ_H. This tendency was seen mainly on the Pt/WC surfaces, where the difference between molecular hydrogen adsorption energies at the lowest (1/8 ML) and highest (1 ML) Θ_H are ~ 0.55 and 0.20 eV for the C-WC and W-WC terminations, respectively. This drop in the adsorption energy is mainly due to the increasing repulsive interaction of H_2 with pre-adsorbed atomic hydrogen, already present on the surface, discussed above.

Another interesting feature seen from adsorption energies in Fig. 2, is that on Pt(111) and on Pt/Mo-Mo_2C, the presence of atomic hydrogen stabilizes the molecular adsorption of H_2. This suggests that the variations in the H_2 adsorption strength on the Pt/TMC surfaces seen at different surface coverages, could originate from the electronic structure of the supported Pt monolayer. Indeed, the analysis of the *d*- band position for the Pt ML (indicated below), evidences that in all the Pt/TMC systems the shift towards more negative values have been observed.[21] However, on the surfaces where a weakening of the H_2—Pt interaction has been observed, a significant *d*-band center downshift is seen relative to that of Pt(111) (-2.58 eV): -3.44 eV for Pt/C-WC, -3.01 eV

for Pt/W-WC and -3.30 eV for Pt/C-Mo_2C. At the same time the *d*-band center for Pt monolayer in the Pt/Mo-Mo_2C system is located at -2.63 eV, being very close to the *d*-band center of the unsupported Pt(111), resulting in a similar response of the molecular hydrogen adsorption energy to the surface coverage, seen on these surfaces.

3.3 H_2 dissociation on Pt/TMC surfaces

H_2 occupies top sites on all the Pt/TMC surfaces. As for atomic H, its stable adsorption site is more surface-specific (See Fig. S1): C*hcp* on Pt/C-Mo_2C, Mo*hcp* – on Pt/Mo-Mo_2C, C*hcp* – on Pt/C-WC and top – on Pt/W-WC.[21] Using stable geometries of H_2 and H on all Pt/TMC surfaces at lowest (1/8 ML), intermediate (1/2 ML) and highest (1 ML) hydrogen coverages, dissociation barriers were calculated (Fig. 3). As a benchmark, the dissociation barriers on Pt(111) were also calculated at the intermediate (highest) hydrogen coverage, using an initial state where H_2 weakly adsorbs atop of platinum atom and six (fourteen) hydrogen atoms simultaneously occupy E*hcp* (fcc) sites;[21] the final state corresponded to eight (sixteen) hydrogen atoms occupying the E*hcp* (fcc) sites.

At the lowest 1/8 ML coverage, no barrier was found for H_2 dissociation on Pt(111) and Pt/C-WC surfaces. For this particular later system, the barrierless dissociation can be explained by analyzing the H—H bond length found upon the stable H_2 adsorption on the Pt/TMC surfaces (see Table S2 and Fig. 2). It is evident that the value of 0.90 Å, found for the Pt/C-WC system, is the largest compared to those on the rest of the TMC-supported Pt monolayers. Thus, it is possible that the H_2 adsorption on the pristine Pt/C-WC surface is not entirely “intact”, and the molecule gets activated while coming closer to the surface.

The absence of the transition state (TS) for H_2 dissociation on Pt/C-WC surface was confirmed by the vibrational frequencies analysis that showed only non-imaginary frequencies present in the system, while a single imaginary frequency (which is a unique property of a TS) has not been found for any of the intermediate images.

As for Pt(111) without atomic hydrogen present on the surface, taking into account the high mobility of molecular hydrogen,[13,73] it can be argued that H_2 might be able to enter a state where the H—H distance is sufficient enough that further separation of its H atoms will occur without a noticeable energy barrier. Additionally, the high mobility of atomic H on Pt(111),[19] may further facilitate the barrierless dissociation.

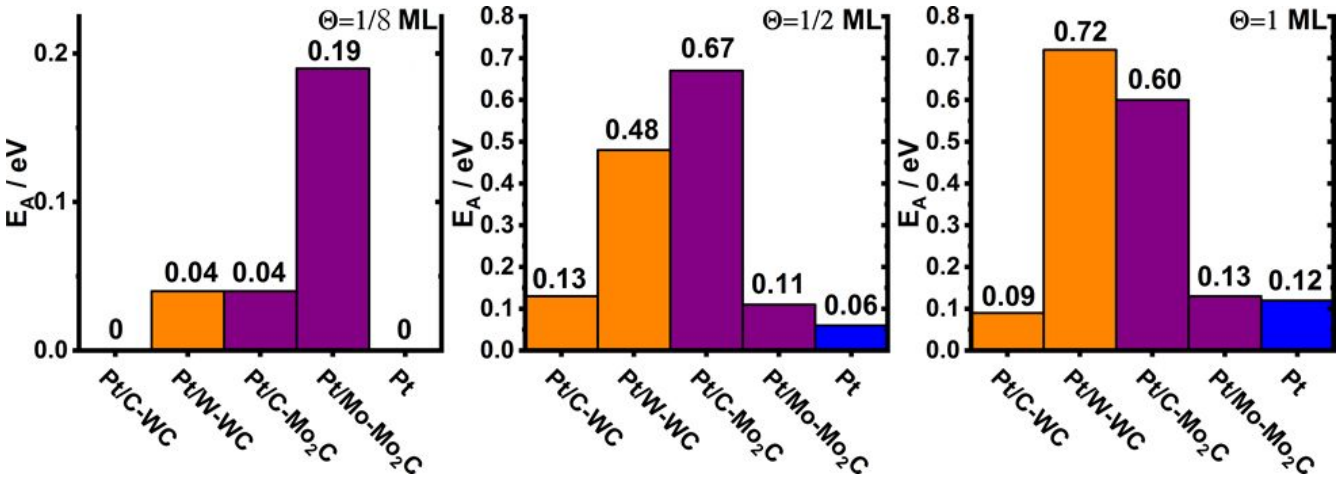

Fig. 3. Energy barriers (E_A) calculated for the $H_2 \rightarrow 2H$ process on the Pt/TMC systems and Pt(111) at different hydrogen surface coverages.

At the same 1/8 ML coverage, the dissociation barriers on the remaining Pt/W-WC, Pt/C-Mo_2C and Pt/Mo-Mo_2C surfaces are rather low. In all cases, a single transition state is represented by an elongation of the H—H distance and mutual reorientation of the hydrogen atoms towards their locations after the dissociation.

Low dissociation barriers calculated on the Pt/TMC at the 1/8 ML surface coverage are in good agreement with the H—H distances in the H_2 molecule adsorbed on the Pt/W-WC, Pt/Mo-Mo_2C and Pt/C-Mo_2C. These values are larger than of 0.75 Å (bond length in gas phase), indicating an activation of molecular hydrogen upon its adsorption on clean (without any pre-adsorbed atomic H) Pt/TMC.

With hydrogen coverage increasing from Θ_H =1/8 to 1/2 ML, additionally to a low barrier on Pt/Mo-Mo_2C (0.11 eV), small barriers appear for H_2 dissociation on Pt/C-WC and Pt(111) (0.13 and 0.06 eV, respectively). In contrast, the barriers are significantly larger on Pt/W-WC (0.48 eV) and Pt/C-Mo_2C (0.67 eV).

Analyzing the geometries of the IS, TS and FS for H_2 dissociation on Pt(111), Pt/C-WC and Pt/Mo-Mo_2C at the intermediate 1/2 ML coverage (Fig. 4), it can be seen that in all systems, the transition state geometry corresponds to the molecule reorientation, so that its atoms come closer to nearest available stable adsorption site for atomic hydrogen. In case of Pt and Pt/C-WC a shortening of the Pt—H_2 distance is seen as well from more than 3 Å (Table S2) to ~2.20 Å, while on Pt/Mo-Mo_2C surface no significant change in the Pt—H_2 distance is seen do to the short initial Pt-H_2 distance on this surface.

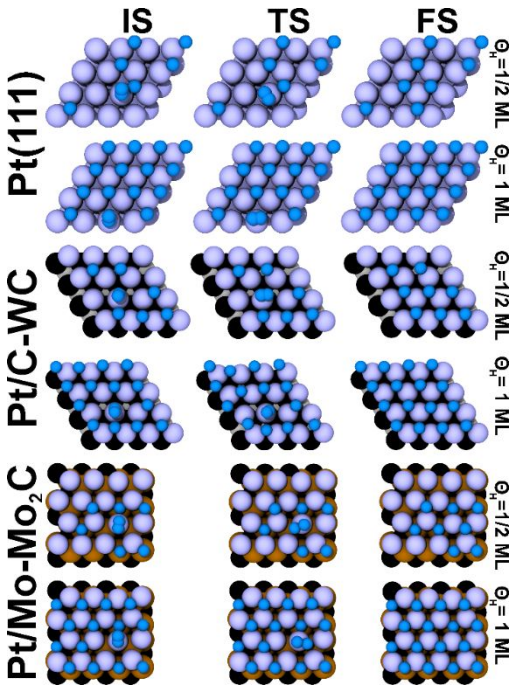

Fig. 4. Geometry structures for initial, transition and final states for H_2 dissociation on Pt(111), Pt/C-WC and Pt/Mo-Mo_2C surfaces at intermediate 1/2 ML and high 1 ML coverages. Spheres color code is the same as in Fig.s 1 and 2.

The same Pt/C-WC and Pt/Mo-Mo_2C surfaces, show a behavior similar to that of Pt towards molecular hydrogen dissociation at the highest 1 ML hydrogen coverage. The main difference is that on Pt/C-WC surface, the TS geometry corresponds to molecule of hydrogen still separated by the distance of 2.80 Å from the surface (significantly larger than 2.20 Å observed in the TS on this surface at Θ_H=1/2 ML), while on Pt(111) and Pt/Mo-Mo_2C the Pt—H_2 distances do not change significantly with the coverage increasing from 1/2 ML to 1 ML. Therefore, we conclude that on Pt/C-WC the molecule experiences more repulsive interaction from the atomic hydrogen present on the surface than on unsupported platinum and on Pt/Mo-Mo_2C, in agreement with trends seen for H_2 adsorption energies seen in Fig. 2.

Overall, for all the studied surfaces, the height of the barrier does not change significantly while increasing the coverage from 1/2 to 1 ML, except for Pt/W-WC. The geometry of the TS at these coverages corresponds to the H_2 molecule coming closer to the surface with the simultaneous increase of the H—H bond length to the values between 0.9 and 1.3 Å (see Table 1).

From the close analysis of the dissociation barriers on the TMC-supported platinum monolayer, together with the initial and final geometries, it can be argued that the barrier height is defined by the initial H—H bond length in the H_2 molecule on the surface, *i.e.* if it gets activated upon interaction with a Pt/TMC. Another important factor is the location of the site for the resulting atomic H relative to the stable site for H_2 adsorption. If the separation between these sites were significant, more energy would be required to move the hydrogen atoms

in H_2 molecule. Additionally, at the coverages 1/2 and 1 ML the movement of the atomic H on the surface will be hindered by the repulsive interaction with H atoms already present on the surface.

Interestingly, while for Pt(111) the orientation of hydrogen molecule to the surface is an important factor, determining the presence or absence of a dissociation barrier,[67] it does not play a significant role in the case of H_2 dissociation on Pt/TMC. Indeed, it can be seen in Fig. S2 that, even when the H_2 molecule is almost perpendicular to the Pt/C-WC surface at the intermediate and highest coverage, the dissociation barriers constantly remain low (Fig. 3). At the same time on Pt/W-WC, the H_2 molecule is found parallel to the surface at all hydrogen coverages, however the dissociation barriers are quite high.

Thus, at low surface coverage, the H_2 molecule is able to come close enough to the Pt/TMC surfaces to get activated and the absence of the surface atomic hydrogen would allow H_2 dissociation onto the closest sites available (Fig. S1), reducing the contribution of the site separation between the initial molecular hydrogen and resulting atomic hydrogen into the barrier height. As a result, little or entirely absent dissociation barriers are observed at Θ_H =1/8 ML for all the studied systems.

At the intermediate 1/2 ML coverage, some sites on the surfaces preferable for atomic H adsorption, get occupied. Hence, the effect of the separation between the locations of the reactant and products on the barrier height would be more obvious. For Pt/W-WC system in which H_2 and atomic H both adsorb on top of Pt atom, the separation is $\sim$ 3 Å (Fig. S1) which leads to 0.48 eV barrier on this surface, that further grows when more H atoms are present on the surface. In other words, increasing the hydrogen surface coverage affects the kinetics of H_2 dissociation.

On the Pt/C-Mo_2C surface the barrier at Θ_H =1/2 ML is the highest observed for this system at all coverages due to the very specific way that atomic H adsorbs on this surface. The most stable adsorption site for H atom in this system is the C*hcp*, where it interacts with the carbon atom of the carbide support located underneath of the Pt ML (see Fig. 2). Before these sites get saturated, atomic H would adsorb exclusively on them. If some of the closest C*hcp* sites would be already occupied by the surface hydrogen, after the H—H bond cleavage both H atoms would need to move to the closest unoccupied C*hcp* site that may be separated significantly (Fig. S1), resulting in a high barrier.

Another limiting factor here is the geometry of H adsorption on this surface. Upon occupation of the C*hcp* site, it "yanks" the C atom from underneath of the supported monolayer in the Pt/C-Mo_2C system[21] (See Fig. S2). This rather significant alteration of the geometry of the surface is specific to this particular system. In the sense that the adsorbate interacting with the support is somewhat similar to hydrogen migration from the metal catalyst particle onto the catalyst support (spillover), reported for platinum supported on a series of substrates.[77-80] Nonetheless, the principal difference between the phenomena observed in the H-Pt/C-Mo_2C system and

during the spillover is that in former case, the H atom remains above the surface plane and pulls a carbon atom of the support through the adlayer; while in the latter, it is either incorporated into the adlayer or comes below it. To our knowledge hydrogen spillover has not been reported for WC- and Mo_2C-supported platinum systems and thus, insertion of hydrogen between the adlayer and substrate is not likely for the considered surfaces.

This process while not being restricted by the geometry of the Pt monolayer at 1/8 ML surface coverage, and thus not affecting significantly the height of the dissociation barrier, at the higher coverages would gradually grow hindered with each hydrogen atom added to the surface and upon reorganization of the Pt monolayer associated with their presence.

Thus, even if dissociation is taking place with the resulting H atoms moving to the C*hcp* sites closest to the original top site, the increased deformation of the Pt adlayer, seen in Fig. S1, would make the accommodation of the resulting two atoms of hydrogen more problematic, since one of them would need to overcome an increased separation between the initial and final locations, caused by the atomic hydrogen-induced deformation of the surface (Fig. S1).

Consequently, at the higher 1 ML coverage, all the C*hcp* sites get saturated by atomic H, and the products of the dissociation can occupy other stable sites on the surface, including those in the vicinity of the initial adsorption location of the hydrogen molecule as seen in Fig. S1, thus slightly lowering the dissociation barrier from 0.72 eV at 1/2 coverage to 0.60 eV at Θ_H=1 ML.

As for the systems with lowest barriers at all coverages, *i.e.* Pt/C-WC and Pt/Mo-Mo_2C, atomic hydrogen preferably adsorbs on the three-fold hollow sites of these surfaces, close to the stable location of the H_2 molecule (see Fig. S1). Atomic hydrogen presence on these surfaces does not cause a significant deformation, and the separation of the initial and final sites remains more or less the same at all Θ_H. Thus, the H atoms would not require to overcome a large distance from the initial to final location, and, therefore, their repulsive interaction with the surface H atoms would be minimal, resulting in the observed low barriers, similar to Pt(111), where the most stable atomic hydrogen adsorption is also seen on the similar three-fold hollow location.

Taking a look at the calculated barriers for the reverse reaction ($E_{a,rev}$) $2H \rightarrow 2H_2$ in Table S2, it is clear that on most of the surfaces hydrogen dissociation is irreversible, with the exception of three particular cases: a) Pt/W-WC at intermediate 1/2 ML coverage (E_a=0.48 vs $E_{a,rev}$=0.21 eV), b) Pt/W-WC at the highest 1 ML coverages (E_a=0.72 vs. $E_{a,rev}$=0.04 eV) , and c) Pt/C-Mo_2C at the highest Θ_H=1 ML (E_a=0.60 vs. $E_{a,rev}$=0.38 eV). In these systems the dissociation of the H_2 molecule is restricted, since activation energy for the reverse reaction of hydrogen formation is lower than the barrier for the dissociation process. For the Pt/W-WC surface this is explained by the combination of two factors, discussed above: both significant separation of the stable adsorption sites for atomic and molecular hydrogen and repulsive interaction between surface hydrogen atoms, hinder significantly accommodation of the reaction products (atomic H) on the surface. For Pt/C-Mo_2C the lack of the preferable

C*hcp* sites at Θ_H=1 ML is the main factor restricting H_2 dissociation on this surface, leading to increased repulsive H-H interactions and impeding the adsorption of the products of H_2 dissociation on the surface.

Another particular case is Pt/C-Mo_2C at the intermediate 1/2 ML coverage, where the barrier for hydrogen formation is the highest ($E_{a,rev}$=2.70 eV), which is the result of a very stable H-surface interaction in this system, taking place exclusively through formation of C—H covalent bonds, making separation of atomic H from the surface energetically not favorable.

Thus, the results evidence that additionally to stabilizing the molecular hydrogen, the presence of the TMC support has a remarkable impact on H_2 dissociation. From the point of view of the height of the barriers, both supports have a termination on which platinum adlayers show dissociation of H_2 in a fashion similar to that of Pt(111): Pt/C-WC and Pt/Mo-Mo_2C. These systems can be used as a potential and cheaper option to pure Pt(111), effectively removing its costly bulk part and optimizing the use of the monolayer in contact with hydrogen.

3.4 Reaction rates for H_2 dissociation at different temperatures

Reaction energies

Detailed information on the H_2 dissociation reaction rates on the Pt/TMC and Pt(111) surfaces at 298 K is summarized in Table 1.

At the lowest coverage Θ_H = 1/8 ML the reaction is exothermic on all surfaces. Total energy of H_2 dissociation on Pt(111) is almost twice as high as on the Pt/C-Mo_2C, where the dissociation is the most exothermic, compared to the rest of the Pt/TMC surfaces in the same conditions.

The trend in the reaction energy for the lowest coverage (Θ_H =1/8) is as follows: Pt(111) > Pt/C-Mo_2C > Pt/W-WC > Pt/C-WC > Pt/Mo-Mo_2C. This trend changes somewhat, with the Θ_H increasing from 1/8 to 1/2 ML. At this intermediate coverage, the reaction energy on Pt(111) points to a decrease in its exothermic nature. On the Pt/C-Mo_2C system, the reaction energy is very high due to the formation of the strong C—H covalent bonds between the C atoms of the support on the C*hcp* sites and atomic H, resulting from the H_2 dissociation. However, the dissociation on Pt/C-Mo_2C is kinetically restricted, since the energy barrier is the highest (0.67 eV) among the studied surfaces at Θ_H =1/2.

At the same time, the dissociation on Pt/W-WC surface becomes endothermic because the addition of two more H atoms to those already adsorbed on the surface, causes weakening of the H—surface interaction seen from the decreasing adsorption energy of each added H atom on this surface.[21] Thus, at Θ_H =1/2 ML, the reaction energy is decreasing in the order Pt/C-Mo_2C > Pt(111) > Pt/C-WC > Pt/Mo-Mo_2C > Pt/W-WC.

Finally at the highest surface coverage the reaction is most exothermic on the Pt(111) surface, while for the Pt/W-WC it is the most endothermic, due to the weakening of the H—surface interaction.[21] An interesting effect related to the preferable adsorption sites for H was observed on the reaction energy on Pt/C-Mo_2C surface. As discussed above, an exhaustion of the extremely stable C*hcp* sites after Θ_H =1/2 ML, where the reaction is still exothermic, leads to an occupation of the next stable sites on the surface (a similar behavior was seen in other systems[9,76]), leading to an endothermic H_2 dissociation in this system at 1 ML surface coverage. Therefore, the order in which the H_2 dissociation reaction energy decreases is Pt(111) > Pt/C-WC > Pt/Mo-Mo_2C > Pt/C-Mo_2C > Pt/W-WC.

It can be seen that the Pt/C-WC and Pt/Mo-Mo_2C were the systems where the reaction energy at the intermediate and highest surface coverages is high (together with low energy barriers), only being outperformed by Pt(111).

Table 1. H_2 dissociation activation barriers (E_a), reaction rates at 298 K (r), reaction energy (ΔE), H—H distance in the TS ($d_{H—H}$) and its imaginary frequency (ν_{im}).

Surface	E_a / eV	r / s^{-1}	ΔE / eV	$d_{H—H}$ / Å	ν_{im} / cm^{-1}
Θ_H =1/8 ML					
Pt/C-Mo_2C	0.04	3.79×10^{13}	-0.59	1.24	815
Pt/Mo-Mo_2C	0.19	3.14×10^{10}	-0.23	0.92	267
Pt/C-WC	0	–	-0.36	–	–
Pt/W-WC	0.04	1.59×10^{12}	-0.49	1.17	810
Pt(111)	0	–	-1.08	–	–
Θ_H =1/2 ML					
Pt/C-Mo_2C	0.67	4.36×10^{6}	-2.03	0.97	288
Pt/Mo-Mo_2C	0.11	1.10×10^{11}	-0.14	1.30	788

Pt/C-WC	0.13	2.61×10^{10}	-0.64	1.19	577
Pt/W-WC	0.48	3.94×10^{8}	0.27	1.21	657
Pt(111)	0.06	1.94×10^{11}	-0.86	0.93	276
Θ_H =1 ML					
Pt/C-Mo_2C	0.60	64.54×10^{6}	0.21	1.16	910
Pt/Mo-Mo_2C	0.13	3.57×10^{10}	-0.10	1.31	816
Pt/C-WC	0.09	1.52×10^{11}	-0.25	1.01	331
Pt/W-WC	0.72	3.54×10^{6}	0.68	1.08	450
Pt(111)	0.12	2.59×10^{10}	-0.78	0.86	309

Reaction rates

In agreement with very low barriers seen at the lowest coverage on all surfaces (where the intact H_2 adsorption is possible), the reaction rates are very high at 298 K (Table 1). The highest reaction rate was observed on the Pt/C-Mo_2C surface, while on the Pt/Mo-Mo_2C it is three orders less, and on the Pt/W-WC the reaction occurs ten times slower than on Pt/C-Mo_2C. The H_2 dissociation rates on Pt(111) and Pt/C-WC were not evaluated due to the absence of the barrier in these systems at Θ_H=1/8 ML.

At the same temperature and surface coverage increasing to the intermediate 1/2 ML, the reaction rate on Pt/C-Mo_2C and Pt/W-WC decreased, which is due to an increase in the H_2 dissociation barriers in these systems. This is especially obvious for the Pt/C-Mo_2C system, where its value is low ($4.36\text{x}10^{6}$ s^{-1}), as compared to other rates in the order from 10^{8} to 10^{11} s^{-1}. On the remainder of the surfaces, including Pt(111), the dissociation barriers are significantly lower and reaction rate remains very high. At this coverage, the rate of the reaction on the Pt/Mo-Mo_2C is the closest to that on Pt(111), compared to the rest of the TMC-supported Pt monolayers. Therefore, at Θ_H =1/2, the Pt/Mo-Mo_2C surface has a Pt-like behavior in terms of both energy barriers and reaction rates at 298 K.

Keeping the same temperature of 298 K and further increasing the coverage to 1 ML leads to a slight improvement the reaction rate on the Pt/C-Mo_2C surface. However, on the Pt/W-WC, the rate deteriorates and becomes the lowest compared to that on the rest of the Pt/TMC surfaces, which is due to the significant increase

of the dissociation barrier as explained above. As in case of the 1/2 ML surface coverage Pt/Mo-Mo_2C is the closest, rate-wise, to the pure unsupported Pt(111). Therefore, at 1 ML Θ_H, the hydrogen dissociation reaction characteristics on Mo-Mo_2C surface are the most similar to those on Pt at 298 K. Nonetheless, molecular hydrogen dissociation on these surfaces is not the fastest one, since the rate is the highest on Pt/C-WC, due to the lowest barrier on this surface at this coverage.

Finally, we studied the dependence of dissociation rate on temperature in the range of from 298 to 1200 K on all the studied surfaces (see Fig. 5). At the lowest coverage of 1/8 ML the rate of dissociation increases on all surfaces (where a barrier is present) with the temperature. However, the highest growth was observed on Pt/C-Mo_2C, 10 to 130 times higher (in the temperature range), as compared to the rate increase on Pt/Mo-Mo_2C and Pt/C-WC. This is due to the specific nature of the preferable adsorption sites for atomic hydrogen on Pt/C-Mo_2C and a strong C-H bond formation, as discussed above. As of the metal polar Mo- and W-terminations they show a low increase in reaction rates as temperature increases.

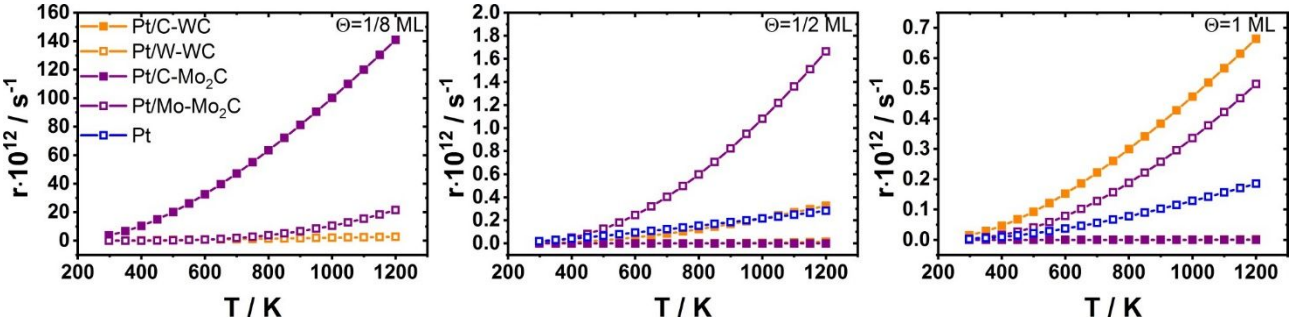

Fig. 5. Temperature effect on the H_2 dissociation rates on Pt/TMC systems at different surface coverages. The Pt(111) surface is shown as well for comparison.

Significantly more interesting trends are seen at the intermediate coverage (Θ_H =1/2 ML). The surfaces on which the dissociation occurs with a high barrier, *i.e.* Pt/C-Mo_2C and Pt/W-WC (on the latter surface the reverse reaction is even more probable) do not show a noticeable rate increase in the whole range of temperatures. Also, for the Pt/C-Mo_2C surface, the saturation of the available C*hcp* sites, where the most stable H adsorption takes place, is an additional limiting factor for an increase in the reaction rate with the temperature.

At the intermediate coverage the highest increase in reaction rate was observed on Pt/Mo-Mo_2C, being almost twice relative to that seen on the Pt(111) surface. The increase of the dissociation rate with temperature

on Pt(111) and Pt/C-WC surfaces at Θ_H =1/2 ML is smaller than on the Pt/Mo-Mo_2C, even despite the dissociation barrier on this latter surface being twice as high as on Pt(111), indicating an improvement in the catalytic behavior of Pt/Mo-Mo_2C as compared to that of Pt(111).

At the highest 1 ML coverage, the reaction rate does not change significantly on Pt/C-Mo_2C and Pt/W-WC, mainly due to the fact that the reverse reaction of hydrogen formation is more probable on these surfaces. On Pt/C-Mo_2C, the C*hcp* sites are now completely blocked by atomic hydrogen and the products of dissociation need to accommodate on the next preferable locations. While some of these sites being located close to the initial position of the H_2 molecule, resulting in a dissociation barrier slightly lower than on the same surface at Θ_H =1/2 ML as was discussed above, nonetheless it is not enough to give a rise to a noticeable increase of the reaction rate with growing temperature. Similarly, for Pt/W-WC the significant separation between the locations of the reactant and products reduces the effect of the temperature on the reaction speed. At the highest surface coverage (Θ_H =1), the Pt/Mo-Mo_2C and Pt/C-WC systems have an improved behavior as compared to Pt(111), since the reaction rates on the complex surfaces increase with the temperature significantly faster than on Pt(111).

The reaction rate response to the increasing temperature on Pt(111) does not change significantly going from 1/2 ML to 1 ML coverage. The same cannot be said about the Pt/Mo-Mo_2C surface, where at Θ_H =1/2 ML the observed rate increase was significantly higher than at 1 ML coverage. Nonetheless, this system is the closest to the unsupported Pt(111) in its properties for the H_2 dissociation as suggested by similar barriers at the intermediate and high surface coverage and comparable trends in H_2 stability at the same coverages. The Pt/C-WC surface, although showing some similarities to Pt(111) and Pt/Mo-Mo_2C surfaces in the way how the H_2 dissociation occurs on them, also shows a different response of the reaction rate to the temperature. Thus, both nature of the support, and its polar termination (C, W, Mo), have a fundamental impact on the H_2 dissociation reaction properties taking place on the supported Pt monolayers.

4 Conclusions

Periodic DFT calculations have been carried out to investigate molecular hydrogen adsorption and dissociation on pristine and H-covered Pt monolayers (hydrogen surface coverages), supported on α-WC(0001) and β-Mo_2C(100) surfaces, considering polar C-, W-, and Mo-terminations. The obtained information demonstrates that the TMC support induces noticeable changes in the structural and electronic properties of the supported platinum monolayer, which in turn define how the resulting Pt/TMC material interacts with molecular

and atomic hydrogen. The characteristics of the hydrogen dissociation reaction also depend on the nature of the TMC acting as support, and on the extent of the hydrogen surface coverage.

The present study evidences that at the lowest hydrogen surface coverage Pt/TMC systems, the interaction with hydrogen molecule is very similar to that on Pt(111), since in all of them a dissociative adsorption of H_2 is observed, however, intact adsorption of H_2 (without H-H bond scission) is possible on the Pt/TMC and is not seen on Pt(111).

Very small barriers accompany molecular hydrogen dissociation on all Pt/TMC, except for Pt/C-WC, at the low coverage. Their heights depend on the hydrogen surface coverage, structure of the supported Pt monolayer and the nature of the TMC support.

Characteristics of the dissociation reaction, such as its energy, rate, and its response to temperature rise at any surface coverage, also depend heavily on the TMC supporting the Pt monolayer. Notably, both α-WC(0001) and β-Mo_2C, have a termination at which the supported monolayer shows catalytic properties towards hydrogen dissociation comparable to those on Pt(111): Pt/Mo-Mo_2C and Pt/C-WC. On the contrary, the surfaces Pt/C-Mo_2C and Pt/W-WC are not suitable for H_2 dissociation.

The observations made in the present work may lay a basis for a better understanding of the complex Pt/TMC systems in the context of their applications in heterogeneous catalysis and can offer a way for a fine tuning of the catalytic properties of the resulting Pt/TMC systems for hydrogen dissociation and other chemical processes significant for *green* energy production and storage.

Declaration of Competing Interest

The authors declare that they have no known competing financial interests or personal relationships that could have appeared to influence the work reported in this paper.

Acknowledgments

Authors would like to thank Universidad de Medellín, UdeM, (A. Koverga, E. Florez, and C. Jimenez-Orozco), for the financial support. Part of this research used resources of the Center for Functional Nanomaterials (J. A. Rodriguez), which is a U.S. DOE Office of Science Facility, and the Scientific Data and Computing Center, a component of the Computational Science Initiative, at Brookhaven National Laboratory under Contract No. DE-SC0012704.

Appendix A: Supplementary Information

Supplementary material related to this article can be found, in the online version, at doi:

References

1. J. N. Wilson, J. W. Otvos, D. P. Stevenson and C. D. Wagner, *Ind. Eng. Chem.*, 1953, **45**, 1480–1487.
2. R. B. Levy and M. Boudart, *Science*, 1973, **181**, 547–549.
3. H. H. Hwu and J. G. Chen, *Chem. Rev.,* 2005, **105**, 185–212.
4. T. G. Kelly, S. T. Hunt, D. V. Esposito and J. G. Chen, *Int. J. Hydrog. Energy*, **38**, 5638–5644.
5. D. V. Esposito, S. T. Hunt, Y. C. Kimmel and J. G. Chen, *J. Am. Chem. Soc.* 2012, **134**, 3025–3033.
6. Daily Metal Prices, https://www.dailymetalprice.com, (accessed August 2021).
7. D. V. Esposito, S. T. Hunt, A. L. Stottlemyer, K. D. Dobson, B. E. McCandless, R. W. Birkmire and J. G. Chen, *Angew. Chem., Int. Ed.*, 2010, **49**, 9859–9862.
8. J. R. dos S. Politi, F. Viñes, J. A. Rodriguez and F. Illas, *Phys. Chem. Chem. Phys.*, 2013, **15**, 12617.
9. C. Jimenez-Orozco, E. Flórez, F. Viñes, J. A. Rodriguez and F. Illas, *ACS Catal.*, 2020, **10**, 6213–6222.
10. C. J. Heard, C. Hu, M. Skoglundh, D. Creaser and H. Grönbeck, *ACS Catal.*, 2016, **6**, 3277–3286.
11. K. Christmann, G. Ertl and T. Pignet, *Surf. Sci.*, 1976, **54**, 365–392.
12. P. Samson, A. Nesbitt, B. E. Koel and A. Hodgson, *J. Chem. Phys.*, 1998, **109**, 3255–3264.
13. B. Poelsema, K. Lenz and G. Comsa, *J. Condens. Matter Phys.*, 2010, **22**, 304006.
14. A. C. Luntz, J. K. Brown and M. D. Williams, *J. Chem. Phys.*, 1990, **93**, 5240–5246.
15. A. T. Gee, B. E. Hayden, C. Mormiche and T. S. Nunney, *J. Chem. Phys.*, 2000, **112**, 7660–7668.
16. G.-J. Kroes and C. Díaz, *Chem. Soc. Rev.*, 2016, **45**, 3658–3700.
17. J. Ludwig, D. G. Vlachos, A. C. T. van Duin and W. A. Goddard, *J. Phys. Chem. B*, 2006, **110**, 4274–4282.
18. P. Ferrin, S. Kandoi, A. U. Nilekar and M. Mavrikakis, *Surf. Sci.*, 2012, **606**, 679–689.
19. R. A. Olsen, G. J. Kroes and E. J. Baerends, *J. Chem. Phys.*, 1999, **111**, 11155–11163.
20. J. K. Vincent, R. A. Olsen, G. J. Kroes and E. J. Baerends, *Surf. Sci.*, 2004, **573**, 433–445.
21. A. A. Koverga, E. Flórez, C. Jimenez-Orozco and J. A. Rodriguez, *Electrochim. Acta*, 2021, **368**, 137598.
22. J. Greeley, T. F. Jaramillo, J. Bonde, I. Chorkendorff and J. K. Nørskov, *Nat. Mater.*, 2006, **5**, 909–913.
23. M. E. Björketun, A. S. Bondarenko, B. L. Abrams, I. Chorkendorff and J. Rossmeisl, *Phys. Chem. Chem. Phys.*, 2010, **12**, 10536.
24. J. E. Rekoske, R. D. Cortright, S. A. Goddard, S. B. Sharma and J. A. Dumesic, *J. Phys. Chem.*, 1992, **96**, 1880–1888.
25. R. D. Cortright, S. A. Goddard, J. E. Rekoske and J. A. Dumesic, *J. Catal.*, 1991, **127**, 342–353.
26. A. Salomonsson, M. Eriksson and H. Dannetun, *J. Appl. Phys.*, 2005, **98**, 014505.
27. B. Poelsema, L. K. Verheij and G. Comsa, *Surf. Sci.*, 1985, **152–153**, 496–504.
28. M. Salmeron, R. J. Gale and G. A. Somorjai, *J. Chem. Phys.*, 1977, **67**, 5324–5334.
29. A. S. Kurlov and A. I. Gusev, in *Tungsten Carbides: Structure, Properties and Application in Hardmetals*, Springer International Publishing, Cham, 2013, pp. 191–237.
30. A. A. Koverga, E. Flórez, L. Dorkis and J. A. Rodriguez, *J. Phys. Chem. C*, 2019, **123**, 8871–8883.
31. C. Jimenez-Orozco, E. Florez, A. Moreno, P. Liu and J. A. Rodriguez, *J. Phys. Chem. C*, 2017, **121**, 19786–19795.

32. S. Posada-Pérez, P. J. Ramírez, R. A. Gutiérrez, D. J. Stacchiola, F. Viñes, P. Liu, F. Illas and J. A. Rodriguez, *Catal. Sci. Technol.*, 2016, **6**, 6766-6777.
33. S. Posada-Pérez, P. J. Ramírez, J. Evans, F. Viñes, P. Liu, F. Illas and J. A. Rodriguez, *J. Am. Chem. Soc.* 2016, **138**, 8269–8278.
34. A. A. Koverga, E. Flórez, L. Dorkis and J. A. Rodriguez, *Phys. Chem. Chem. Phys.,* 2020, **22**, 13666–13679.
35. A. A. Koverga, E. Flórez and J. A. Rodriguez, *Int. J. Hydrog. Energy*, 2021, **46**, 25092-25102.
36. A. Tilekaratne, J. P. Simonovis, M. F. López Fagúndez, M. Ebrahimi and F. Zaera, *ACS Catal.*, 2012, **2**, 2259–2268.
37. G. Kresse and J. Hafner, *Phys. Rev. B*, 1993, **47**, 558–561.
38. G. Kresse and J. Furthmüller, *Comput. Mater. Sci.*, 1996, **6**, 15–50.
39. J. P. Perdew, K. Burke and M. Ernzerhof, *Phys. Rev. Lett.*, 1996, **77**, 3865–3868.
40. S. Andresson and M. Grüning, *J. Phys. Chem. A,* 2004, **108**, 7621–7636.
41. E. W. F. Smeets, J. Voss and G. J. Kroes, *J. Phys. Chem. A* 2019, **123**, 5395–5406.
42. M. Wijzenbroek and G. J. Kroes, *J. Chem. Phys.*, **140**, 084702.
43. H. J. Monkhorst, *Phys. Rev. B,* 1979, **20**, 1504.
44. W. Zhong, Y. Qi and M. Deng, *J. Power Sources,* 2015, **278**, 203–212.
45. Y. Sha, T. H. Yu, B. V. Merinov and W. A. Goddard III, *J. Phys. Chem. Lett.* 2010, **1**, 856–861.
46. M. Figueras, R. A. Gutiérrez, F. Viñes, P. J. Ramírez, J. A. Rodriguez and F. Illas, *J. Phys. Chem. Lett.*, 2020, **11**, 8437–8441.
47. P. E. Blöchl, *Phys. Rev. B*, 1994, **50**, 17953–17979.
48. G. Kresse and D. Joubert, *Phys. Rev. B*, 1999, **59**, 1758–1775.
49. S. Posada-Pérez, F. Viñes, P. J. Ramirez, A. B. Vidal, J. A. Rodriguez and F. Illas, *Phys. Chem. Chem. Phys.*, 2014, **16**, 14912–14921.
50. S. Posada-Pérez, F. Viñes, J. A. Rodríguez and F. Illas, *J. Chem. Phys.*, 2015, **143**, 114704.
51. D. D. Vasić, I. A. Pašti and S. V. Mentus, *Int. J. Hydrog. Energy*, 2013, **38**, 5009–5018.
52. J. P. P. Ramalho, J. R. Gomes and F. Illas, *RSC Adv.*, 2013, **3**, 13085-13100.
53. S. Grimme, *J. Comput. Chem.*, 2004, **25**, 1463–1473.
54. S. Grimme, J. Antony, S. Ehrlich and H. Krieg, *J. Chem. Phys.*, 2010, **132**, 154104.
55. H. J. Monkhorst and J. D. Pack, *Phys. Rev. B*, 1976, **13**, 5188–5192.
56. M. Methfessel and A. T. Paxton, *Phys. Rev. B*, 1989, **40**, 3616–3621.
57. G. Henkelman, B. P. Uberuaga and H. Jónsson, *J. Chem. Phys.*, 2000, **113**, 9901–9904.
58. G. Henkelman and H. Jónsson, *J. Chem. Phys.*, 2000, **113**, 9978–9985.
59. I. Chorkendorff and J. W. Niemantsverdriet, in *Concepts of Modern Catalysis and Kinetics,* WILEY-VCH GmbH & Co., 2003.
60. J.K. Nørskov, F. Studt, F. Abild-Pedersen and T. Bligaard, *Fundamental Concepts in Heterogeneous Catalysis,* John Wiley and Sons, Hoboken, 2014.
61. K. Yan, T. A. Maark, A. Khorshidi, V. A. Sethuraman, A. A. Peterson and P. R. Guduru, *Angew. Chem.*, 2016, **128**, 6283–6289.
62. J. R. Kitchin, J. K. Nørskov, M. A. Barteau and J. G. Chen, *Phys. Rev. Lett.*, 2004, **93**, 156801.
63. M. Paßens, V. Caciuc, N. Atodiresei, M. Moors, S. Blügel, R. Waser and S. Karthäuser, *Nanoscale*, 2016, **8**, 13924–13933.
64. H. Duan, Q. Hao and C. Xu, *J. Power Sources*, 2015, **280**, 483–490.
65. B. Hammer and J. K. Nørskov, *Surf. Sci.*, 1995, **343**, 211–220.
66. J. K. Norskov, F. Abild-Pedersen, F. Studt and T. Bligaard, *Proc. Natl. Acad. Sci. U.S.A.*, 2011, **108**, 937–943.
67. N. B. Arboleda, H. Kasai, W. A. Diño and H. Nakanishi, *Jpn. J. Appl. Phys.*, 2007, **46**, 4233–4237.
68. C. Yu, F. Wang, Y. Zhang, L. Zhao, B. Teng, M. Fan and X. Liu, *Catalysts*, 2018, **8**, 450.
69. J. Ludwig and D. G. Vlachos, *Mol. Simul.*, 2004, **30**, 765–771.

70. P. Kraus and I. Frank, *Int. J. Quantum Chem*., 2017, **117**, e25407.
71. S. Posada-Pérez, F. Viñes, R. Valero, J. A. Rodriguez and F. Illas, *Surf. Sci.*, 2017, **656**, 24–32.
72. T. Koido, K. Tomarikawa, S. Yonemura and T. Tokumasu, AIP Conf. Proc., 2011, **1333**, 469–474.
73. B. Poelsema, K. Lenz and G. Comsa, *J. Chem. Phys.*, 2011, **134**, 074703.
74. T. Mueller and G. Ceder, *J. Phys. Chem. B*, 2005, **109**, 17974-17983.
75. F. Silveri, M. G. Quesne, A. Roldan, N. H. de Leeuw and C. R. A. Catlow, *Phys. Chem. Chem. Phys.*, 2019, **21**, 5335–5343.
76. J. J. Piñero, P. J. Ramírez, S. T. Bromley, F. Illas, F. Viñes and J. A. Rodriguez, *J. Phys. Chem. C*, 2018, **122**, 28013–28020.
77. S. Khoobiar, *J. Phys. Chem.*, 1964, **68**, 411–412.
78. S. K. Beaumont, S. Alayoglu, C. Specht, N. Kruse and G. A. Somorjai, *Nano Lett.*, 2014, **14**, 4792–4796.
79. L. R. Merte, G. Peng, R. Bechstein, F. Rieboldt, C. A. Farberow, L. C. Grabow, W. Kudernatsch, S. Wendt, E. Lægsgaard, M. Mavrikakis and F. Besenbacher, *Science*, 2012, **336**, 889–893.
80. B. Li, W. L. Yim, Q. Zhang and L. Chen, *J. Phys. Chem. C*, 2010, **114**, 3052–3058.